Biochimica et Biophysica Acta 1840 (2014) 2234–2243

Contents lists available at ScienceDirect

Biochimica et Biophysica Acta

journal homepage: www.elsevier.com/locate/bbagen

Different activities of the conserved lysine residues in the double-stranded RNA binding domains of RNA helicase A *in vitro* and in the cell

Li Xing *, Meijuan Niu, Xia Zhao, Lawrence Kleiman *

Lady Davis Institute for Medical Research and McGill AIDS Centre, Jewish General Hospital, Montreal, Quebec, Canada
Department of Medicine, McGill University, Montreal, Quebec, Canada

ARTICLE INFO

Article history:
Received 28 October 2013
Received in revised form 2 April 2014
Accepted 3 April 2014
Available online 12 April 2014

Keywords:
HIV-1
RNA helicase A
Double-stranded RNA binding domain
Lysine
Helicase activity

ABSTRACT

Background: RNA helicase A regulates a variety of RNA metabolism processes including HIV-1 replication and contains two double-stranded RNA binding domains (dsRBD1 and dsRBD2) at the N-terminus. Each dsRBD contains two invariant lysine residues critical for the binding of isolated dsRBDs to RNA. However, the role of these conserved lysine residues was not tested in the context of enzymatically active full-length RNA helicase A either *in vitro* or in the cells.
Methods: The conserved lysine residues in each or both of dsRBDs were substituted by alanine in the context of full-length RNA helicase A. The mutant RNA helicase A was purified from mammalian cells. The effects of these mutations were assessed either *in vitro* upon RNA binding and unwinding or in the cell during HIV-1 production upon RNA helicase A–RNA interaction and RNA helicase A-stimulated viral RNA processes.
Results: Unexpectedly, the substitution of the lysine residues by alanine in either or both of dsRBDs does not prevent purified full-length RNA helicase A from binding and unwinding duplex RNA *in vitro*. However, these mutations efficiently inhibit RNA helicase A-stimulated HIV-1 RNA metabolism including the accumulation of viral mRNA and $tRNA^{Lys3}$ annealing to viral RNA. Furthermore, these mutations do not prevent RNA helicase A from binding to HIV-1 RNA *in vitro* as well, but dramatically reduce RNA helicase A–HIV-1 RNA interaction in the cells.
Conclusions: The conserved lysine residues of dsRBDs play critical roles in the promotion of HIV-1 production by RNA helicase A.
General significance: The conserved lysine residues of dsRBDs are key to the interaction of RNA helicase A with substrate RNA in the cell, but not *in vitro*.

1. Introduction

Human RNA helicase A (RHA), also known as DHX9, is a member of DExH-box RNA helicases, and has been reported to promote replication of a number of viruses, such as hepatitis C virus (HCV) [1,2], foot-and-mouth disease virus [3], influenza A virus [4], and HIV-1 [5–8]. While being mainly found in the nucleus, RHA can shuttle back and forth between the nucleus and the cytoplasm [9,10] to participate in a diverse set of cellular processes involving RNA including the activation of transcription [11–14] and stimulation of translation [15]. During HIV-1 replication, RHA preferentially binds the 5′-untranslated region (UTR) of viral RNA [16], and is packaged into viral particles [17]. The enzyme promotes HIV-1 replication at multiple steps including the transcription [5] and translation of viral mRNA [7], and the annealing to viral RNA of $tRNA^{Lys3}$, the primer for reverse transcription of HIV-1 [8].

RHA can unwind double-stranded stretches of both RNA and DNA using any of the four ribo- or deoxyribo-nucleotide triphosphates (NTPs) as energy sources [18,19]. Within the DExH-box family of RNA helicases, RHA uniquely contains two double-stranded RNA binding domains (dsRBDs) N-terminal to the core helicase domain (depicted in Fig. 1A) [20]. The core helicase domain of RHA consists of two subdomains, the DEIH and the HELICc subdomain [21], which is responsible for binding and hydrolyzing NTPs, and is composed of 8 motifs that are conserved in all members of the DExD/H box RNA helicases [22]. The other conserved domains of RHA include the C-terminal RGG domain that contains a stretch of repeated arginine and glycine–glycine residues

Abbreviations: HIV-1, human immunodeficiency virus 1; UTR, untranslated region; RHA, RNA helicase A; dsRNA, double-stranded RNA; ssRNA, single-stranded RNA; NTP, nucleotide triphosphate; nt, nucleotide; dsRBD, double-stranded RNA binding domain; HA2, helicase associated 2; RGG, arginine–glycine–glycine repeats; GST, glutathione S-transferase; OB-fold, oligonucleotide/oligosaccharide binding fold; MLE, RNA helicase maleless; PKR, dsRNA-dependent protein kinase; DGCR8, DiGeorge syndrome critical region gene 8; TRBP, HIV-1 TAR RNA binding protein; ADAR1, adenosine deaminase acting on RNA isoform 1; ADAR2, adenosine deaminase acting on RNA isoform 2

* Corresponding authors at: Lady Davis Institute for Medical Research and McGill AIDS Centre, Jewish General Hospital, 3999 Cote Ste-Catherine Road, Montreal, Quebec H3T 1E2, Canada. Tel.: +1 514 340 8260; fax: +1 514 340 5285.
E-mail addresses: xingli107@gmail.com (L. Xing), lawrence.kleiman@mcgill.ca (L. Kleiman).

http://dx.doi.org/10.1016/j.bbagen.2014.04.003
0304-4165/

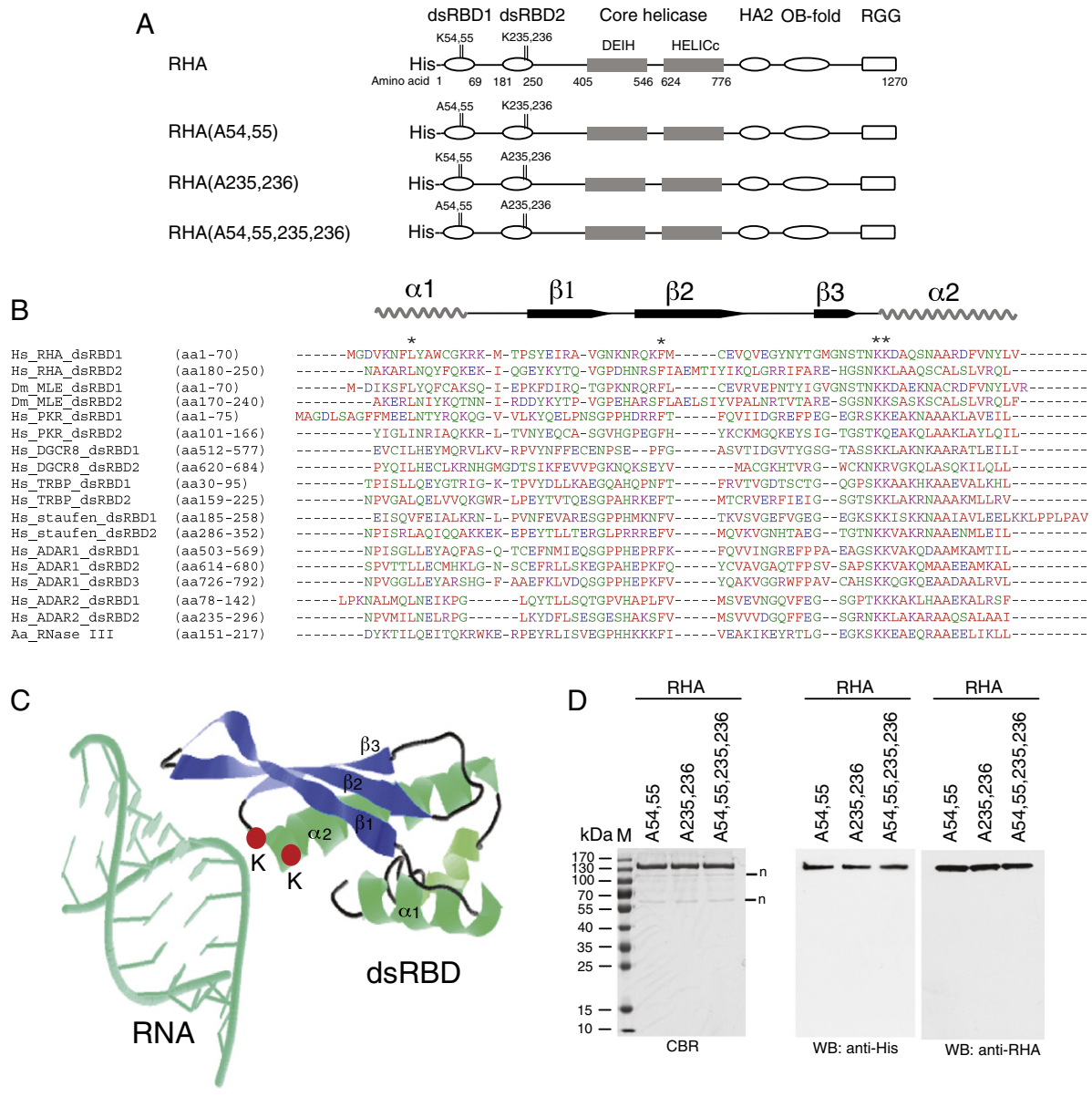

Fig. 1. Purification of mutant full-length RHA. (A) Schematic representation of the domains of wild-type or mutant RHA. The proteins are tagged with 6 × His at the N-terminus. Conserved lysine residues were substituted with alanine residues in dsRBDs of mutant RHAs. (B) Sequence alignment of dsRBDs of various proteins from human being and other organisms including human RHA. *Hs*, *Homo sapiens*; *Dm*, *Drosophila melanogaster*; *Aa*, *Aquifex aeolicus*. Identical or similar residues are in the same color. Asterisks on the top of the letter indicate the highly conserved residues. The secondary structure elements are shown above the aligned protein sequence. (C) Cartoon view of the overall structure of dsRBDs and its interaction with substrate RNA. 3D-domain structure is from human RHA (PDB ID: 3vyy). The red balls indicate the positions of the conserved lysine residues of dsRBD. (D) Purification of mutant full-length RHA. Mutant RHAs were expressed in mammalian cells (293E), purified using Ni-NTA agarose, separated by 1D PAGE, and analyzed by either staining with Coomassie Brilliant Blue R250 (CBR) or Western blotting using anti-His or anti-RHA (WB). M, protein size marker with indicated molecular weights in kDa. n, non-specific protein.

[23–25], the helicase-associated domain 2 (HA2), and the oligonucleotide/oligosaccharide binding (OB)-fold [26]. The function of HA2 and OB-fold of RHA has yet to be investigated.

The dsRBD promotes the interaction of a number of different dsRBD-containing proteins with double-stranded RNA (dsRNA). It usually contains 65–70 amino acids in length (as examples shown in Fig. 1B), and has been found in almost all eukaryotes and most eubacteria [27]. The dsRBD always coexists with other protein domains that confer a variety of functions, such as the adenosine deaminase domain in animal ADAR (adenosine deaminase acting on RNA) [28], RNase III domain in RNase III protein of *Escherichia coli* [29], the kinase domain in human dsRNA-dependent protein kinase (PKR) [30], and the helicase domain in RHA. The three-dimensional structure of isolated dsRBDs from diverse organisms has been determined. Solution structures determined by NMR have been published for dsRBDs from *E. coli* RNase III [31], *Drosophila* Staufen [32,33], the human PKR [34], and the *Saccharomyces cerevisiae* RNase III endonuclease Rnt1p [35,36]. X-ray crystallographic structures have also been developed for dsRBDs of *Xenopus laevis* X1rbpa [37] and human RHA [38] and for the entire RNase III from *Aquifex aeolicus* [39]. As depicted in Fig. 1C, dsRBDs adopt the same α–β–β–β–α topology in which the N- and C-terminal α-helices pack against one face of a three-stranded anti-parallel β-sheet to interact with one face of RNA helix [27].

In a recent study, we found that the deletion of either dsRBD in RHA eliminates the binding of RHA to HIV-1 RNA during virus replication, and results in the inability of RHA to promote the annealing of $tRNA^{Lys3}$ to viral RNA [16]. Like dsRBDs of other proteins, the dsRBDs of RHA also contain conserved lysine residues [27], *i.e.* K54 and K55 in dsRBD1, and

K235 and K236 in dsRBD2 (Fig. 1B). The crystal structure study of either *X. laevis* X1rbpa dsRBD in complex with a 10-nt dsRNA [37] or human RHA dsRBD in complex with a 10-nt GC dsRNA [38] revealed that these basic residues are surface-exposed (Fig. 1C), suggesting their potential roles in the interaction between dsRBDs and target dsRNA. Mutation of these conserved lysines abolished the binding of the isolated dsRBDs to RNA *in vitro* [19,25,38]. However, the role of these conserved lysine residues was not tested in the context of enzymatically active full-length RHA either *in vitro* or in the cell, particularly during HIV-1 production in which RHA participates at the multiple steps of RNA metabolism [40,41]. Unexpectedly, in this report, we found that the mutation of these conserved lysine residues of dsRBDs in the context of full-length RHA does not affect the enzyme's ability to bind RNA *in vitro*, but dramatically reduces the interaction of RHA with HIV-1 RNA during virus production and abolishes the stimulatory effects of RHA upon the accumulation of HIV-1 mRNA and annealing of $tRNA^{Lys3}$ to viral RNA, and significantly reduces the packaging of RHA into virion progeny.

2. Material and methods

2.1. Cell culture

293T, a human embryonic kidney cell line, was grown in Dulbecco's modified Eagle's medium (DMEM, Invitrogen) supplemented with L-glutamine (Gibco), penicillin–streptomycin (Gibco), and 10% fetal bovine serum. HEK 293E cell is a stably transfected HEK 293 cell line [42] that expresses the Epstein–Barr virus nuclear antigen 1 (EBNA1) and promotes the amplification of plasmid pTT5-SH5 containing the replication origin region (OriP) of Epstein–Barr virus, resulting in high expression of proteins coded for by this plasmid.

2.2. Plasmid

SVC21.BH10 is a simian virus 40-based vector that contains full-length wild-type HIV-1 BH10 proviral DNA [43]. All other recombinant plasmids were created by fusion PCR and verified by performing restriction mapping and DNA sequencing. The gel-purified PCR products were digested by NotI and BstEII, and then cloned into parent plasmid pTT5-SH5-RHA [8]. Plasmid pTT5-SH5-RHA contains full-length human RHA coding sequence under control of a CMV promoter, and was also used as a template in PCR. The recombinant plasmids pRHA-A54,55, pRHA-A235,236, or pRHA-A54,55,235,236 encode mutant RHAs in which the conserved lysine residues in dsRBD1, dsRBD2, or both dsRBD1 and dsRBD2 have been replaced by alanine residues. pRHA-A54,55 was generated by fusing PCR product of primer pair RHA-F1(4)/RHA-R(159) to PCR product of primer pair Ala160-F/RHA(BstEII)1026-R. pRHA-A235,236 was generated by fusing the PCR product of primer pair RHA-F1(4)/RHA-R(702) to that of primer pair Ala701-F/RHA(BstEII)1026-R. pRHA-A54,55,235,236 was created by PCR using pRHA-A235,236 as the template, and the same primer pairs used for making pRHA-A54,55. Primers RHA-F1(4) and RHA(BstEII)1026-R have been described [16]. The sequence of other primers used is as follows: RHA-R(159), 5′-ATTGGTGGAATTTCCCAT-3′; RHA-R(702), 5′-ATTTGATCCATGTTCT CG-3′; Ala160-F, 5′-ATGGGAAATTCCACCAATGCCGCCGATGCACAAA GCAATGCT-3′; and Ala701-F, 5′-CGAGAACATGGATCAAATGCCGCC TTGGCAGCACAGTCCTGT-3′.

2.3. Expression and purification of proteins

Mutant RHAs analyzed in this report are N-terminally His-tagged and contain substitution mutation of the conserved lysine residues in the indicated dsRBDs. The expression and purification of mutant RHAs were done as described [8] from HEK 293E cells [44]. Briefly, cells were transfected with indicated plasmids using 25 kDa linear Polyethylenimine (PEI, pH 7.0, Polysciences Inc.), collected 48 h later, washed with ice-cold phosphate-buffered saline, and lysed in buffer containing 50 mM NaH_2PO_4, pH 7.4, 300 mM NaCl, 10 mM imidazole, 0.5% Triton-X 100, 10% glycerol, and protease inhibitor cocktail tablets (Roche). The cell lysates were clarified by centrifugation at 20,000 *g* for 30 min at 4 °C and then incubated with Ni-nitrilotriacetic acid (NTA) agarose (Qiagen) at 4 °C for 2 h to capture His-tagged proteins. After extensive washing, recombinant proteins were eluted by 250 mM imidazole solution (pH 7.4). The purification of N-terminally His-tagged full-length RHA without substitution mutation has been described previously [8] and was referred to as wild-type (WT) in this study. Glutathione S-transferase (GST) was isolated from 293E cells as described previously [16]. The purified proteins were dialyzed against 20 mM Tris–HCl, pH 7.5, 150 mM NaCl, 20 mM KCl, 2 mM $MgCl_2$, 2 mM dithiothreitol, and 10% glycerol and then stored at −80 °C. The purity and the identity of purified proteins were evaluated by Coomassie Brilliant Blue R250 staining and Western blot analysis, respectively. The Bio-Rad protein assay reagent was used to determine protein concentration.

2.4. siRNA and Western blot analysis

Small interfering RNA oligonucleotides $siRNA_{Con}$ and $siRNA_{RHA}$ that was employed to knockdown the endogenous RHA in 293T cells have been described [8]. The level of endogenous RHA was measured by Western blot analysis using anti-RHA. The level of β-actin was measured using β-actin mAb as a sample loading control. Viral or cellular lysates were separated by sodium dodecyl sulfate (SDS)-polyacrylamide gel electrophoresis (PAGE), blotted onto a nitrocellulose membrane, and then probed with appropriate primary antibodies. The membranes were extensively washed and then incubated with horseradish peroxidase-conjugated secondary antibodies (Sigma). After extensive washing again, a chemiluminescence reagent (PerkinElmer) was applied to visualize signals on a Kodak X-ray film. The primary antibodies used in Western blotting include rabbit anti-HIV reverse transcriptase (RTp66/51), mouse anti-p24 [45] (NIH AIDS Research and Reference Reagent Program), β-actin mAb (Sigma), polyclonal rabbit anti-RHA (Novus Biologicals), and poly-histidine mAb (Sigma).

2.5. RNA–protein coprecipitation assay

The RNA–protein coprecipitation assay was developed to pull-down RNA/protein complexes, and was performed as described [16]. Briefly, 293T cells were cotransfected with SVC21.BH10 and a plasmid expressing His-tagged wild-type or mutant RHA. 24 h later, cells were cross-linked in 1% formaldehyde (Bioshop), lysed in lysis buffer (50 mM Tris–HCl, pH 7.5, 150 mM KCl, 1% NP-40, 0.1% SDS, 0.5% sodium deoxycholate, 50 mM NaF, 1000 U/ml SUPERase-in [Ambion], and protease inhibitor cocktail tablets [Roche]), and sonicated. After centrifugation, the clear supernatants were incubated with salmon sperm DNA and mammalian RNA-saturated Ni-NTA agarose to capture His-tagged proteins. After extensive washing, the captured protein was eluted with 250 mM imidazole, pH 7.4, reverse cross-linked, analyzed by Western blotting, and then extracted with TRIzol reagent (Life technology) to isolate RNA. The RNA sample was treated with DNase and then subjected to semiquantitative RT-PCR analysis. The total RNA (2%) was isolated before incubation with Ni-NTA agarose as an input control.

2.6. RT-PCR

Reverse transcription reaction was carried out to synthesize cDNAs using the Superscript II kit (Invitrogen) and primer P1-R specific for HIV-1 5′-UTR [16]. PCR was then performed using Taq DNA polymerase (Bio Basic Canada). The amplification was started with an initial denaturation at 94 °C for 5 min, followed by 25 cycles at 94 °C for 30 s, 52 °C for 30 s, and 72 °C for 20 s. The final extension was performed at 72 °C for 5 min. The PCR products were separated in 1.5% agarose gel and visualized under UV light after ethidium bromide staining.

2.7. One nucleotide extension assay

The $tRNA^{Lys3}$–viral RNA template was isolated from purified HIV-1 particles as described [46]. The ability of $tRNA^{Lys3}$ annealed *in vivo* to viral RNA to be extended by one nucleotide (dCTP) by reverse transcription was measured in a 20 μl reaction containing 50 mM Tris–HCl, pH 7.8, 100 mM KCl, 10 mM $MgCl_2$, 10 mM dithiothreitol, 0.16 μM [α-^{32}P]-dCTP, 50 ng of HIV-1 RT, and RNase inhibitor (Ambion). After 15 min of incubation at 37 °C, the samples were precipitated with 2-propanol, followed by resolution of the radioactive product on a denaturing 6% polyacrylamide gel. The amounts of extended $tRNA^{Lys3}$ were determined using a PhosphorImager instrument (Amersham Pharmacia Biotech). The amount of viral RNA in the reactions was determined by measuring the ability of a DNA oligonucleotide (5′-TCTAATTCTCCCCC GCTTAATACTGACGCT-3′) annealed at room temperature to the viral RNA sequence downstream of the $tRNA^{Lys3}$ binding site to prime a one nucleotide ([^{32}P]-dCTP) extension.

2.8. Preparation of RNA substrates

The RNA oligonucleotides used to make duplex RNA have been described [47]. The shorter sense RNA strand was labeled with [5′-^{32}P] Cytidine 3′,5′-bis(phosphate) (^{32}pCp) using T4 RNA ligase (Fermentas), and then annealed to cold complementary antisense RNA strand to produce radioactive duplex RNA (diagramed in Fig. 2A). The 100 μl annealing reaction contains equal molar amounts of radioactive and cold complementary RNA in hybridization buffer (20 mM Tris–HCl, pH 7.4, 10 mM $(NH_4)_2SO_4$, 10 mM KCl, 100 mM NaCl, 0.1% Triton X-100) and was incubated at 95 °C for 5 min, at 60 °C for 20 min, and then at room temperature for 20 min. In an electrophoretic helicase assay, the radioactive duplex RNA used was purified by electrophoresis on a 15% native polyacrylamide gel in 0.5 × Tris–borate–EDTA (TBE) and extraction using RNA polygel extraction kit (Biomiga).

2.9. Electrophoretic mobility shift assay (EMSA)

EMSA was carried out to examine the ability of wild-type or mutant RHA to bind dsRNA. 100 nM [^{32}pCp]-labeled synthetic duplex RNA was incubated with increasing amounts of protein (2 nM, 4 nM, 8 nM, 20 nM, and 40 nM) at room temperature for 30 min in 20 μl of binding buffer (20 mM Tris, pH 7.4, 5% glycerol, 50 mM KCl, 10 mM $MgCl_2$, 150 mM NaCl, and 2 mM dithiothreitol). The RNA–protein mixture was loaded onto a 5% native polyacrylamide gel in TBE and then electrophoresed. The gel was then dried and exposed to a PhosphorImager screen. Radioactive signals were detected and analyzed using a PhosphorImager instrument.

2.10. Electrophoretic helicase assay

The helicase activity of mutant RHAs was measured as described [8] in a 20 μl reaction containing 10 mM Tris–HCl, pH 8.0, 50 mM KCl, 2 mM $MgCl_2$, 2 mM dithiothreitol, 2 units of RNasin, 2.5 mM NaH_2PO_4, 15 mM NaCl, 10 nM gel-purified duplex RNA, and, where indicated, 1 mM ATP, and 150 nM purified proteins. The reaction was incubated at 37 °C for indicated time periods and then terminated by adding 5 μl of stop buffer containing 2% SDS, 10 mM $CaCl_2$, 250 μg/ml proteinase K, 40% glycerol, 0.1% bromophenol blue, and 0.1% xylene cyanol. 10 μl of aliquots for each reaction was loaded onto a 15% native polyacrylamide gel in TBE

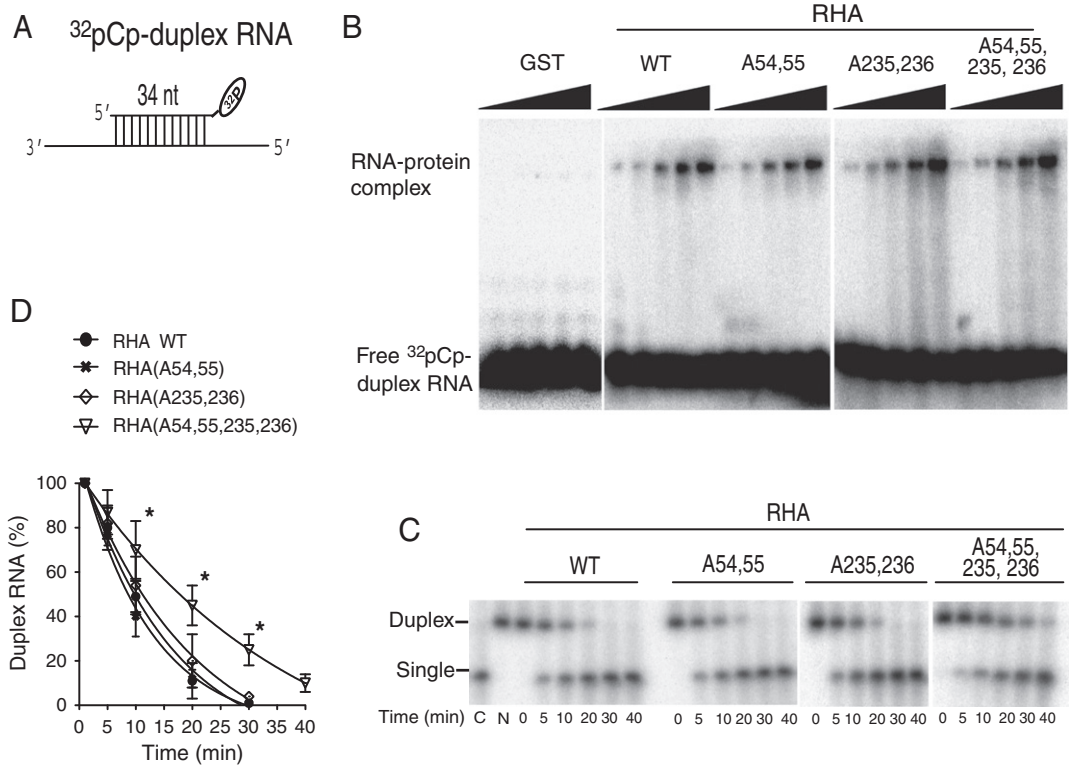

Fig. 2. Effects of mutation of conserved lysine residues on RHA binding to, and unwinding of, dsRNA *in vitro*. (A) Diagram of the duplex RNA. The short RNA strand is 3′-end-labeled with ^{32}pCp. (B) EMSA was carried out to examine the *in vitro* binding of purified proteins to [^{32}pCp]-labeled duplex RNA. Shown is a representative of 3 independent experiments. (C) Helicase activity assay. 10 nM of radioactive duplex RNA was incubated with 150 nM of wild-type or mutant RHA, in the presence or absence of 1 mM ATP, at 37 °C for indicated time periods. The radioactive short RNA strand in single or duplex form was resolved on a 15% native polyacrylamide gel, and visualized using a PhosphorImager instrument. Lane 'C' indicates the migration position of the ssRNA (boiled substrate), while lane 'N' represents the migration position of untreated labeled duplex RNA. Lanes at time point 0 represent the helicase reactions in the absence of 1 mM ATP. Shown is a representative of 3 independent experiments. (D) Duplex RNA bands were quantitated using a PhosphorImager software, normalized to the results obtained at the time point 0, and presented graphically as percentage. Shown are the mean values ± standard deviations (SDs) of 3 independent experiments. *, $P < 0.05$ compared with corresponding values obtained with wild-type RHA.

and then electrophoresed. Radioactive RNAs were visualized and quantitated using a PhosphorImager instrument.

2.11. RNA isolation and Northern analysis

Isolation of total cellular RNA and Northern hybridization were carried out as described previously [48]. 293T cells were cotransfected with SVC21.BH10 and a plasmid expressing His-tagged wild-type or mutant RHAs. Total cellular RNA was prepared using TRIzol reagent 24 h later, and 15 μg RNA per lane was resolved in denaturing 1% agarose–2.2 M formaldehyde gel, transferred onto GeneScreen Plus hybridization transfer membranes (PerkinElmer), immobilized by UV light cross-linking for 5 min, and hybridized with [^{32}P]-labeled DNA probes at 42 °C overnight. [^{32}P]-labeled DNA probes were prepared by using the random primer DNA labeling system (Invitrogen) and DNA template containing sequence of HIV-1 5′-UTR. These probes can recognize all the HIV-1 transcripts produced during virus replication. Membranes were hybridized in ULTRAhyb-Oligo hybridization buffer (Ambion). The signals in Northern blots were detected and quantitated using a PhosphorImager instrument. To monitor the transfection efficiency, the amounts of exogenous RHA-encoding mRNA were assessed by semiquantitative RT-PCR using primer set RHA3′-F(5′-GTTTCCCGAGGT GGCTTTAGAGGC-3′)/pTT-R(5′-CCTTTATTAGCCAGAGGTCGAGGTC-3′). The 3′-UTR of exogenous RHA-encoding mRNA produced from pTT5-SH-RHA or its derivatives was transcribed from the backbone of plasmids, has sequence distinct from that of endogenous RHA-encoding mRNA, and is specifically recognized by primer pTT-R. The 18-mer oligo-(dT) and SuperScript reverse transcriptase III (Invitrogen) were used to synthesize cDNAs from total RNAs. PCR amplification was performed using Taq DNA polymerase with an initial denaturation at 94 °C for 4 min, followed by 20 cycles of 94 °C for 30 s, 52 °C for 40 s, and 72 °C for 30 s, and finalized by an extension at 72 °C for 5 min.

2.12. RNA filter binding assay

The RNA filter binding assay was performed by adapting the double-filter nucleic acid binding assay developed by Wong and Lohman [49]. Briefly, nitrocellulose membranes (Bio-Rad) were presoaked in 0.4 M KOH for 10 min and then rinsed in distilled water until the pH returned to neutral. The membranes were equilibrated in binding buffer (10 mM Tris–HCl, pH 8.0, 50 mM KCl, 2 mM $MgCl_2$, 2 mM dithiothreitol, 2.5 mM NaH_2PO_4, 15 mM NaCl, 4% glycerol) at 4 °C for 1 h before putting on the Whatman paper. The HIV-1 5′-UTR RNA was prepared as described previously [8] and labeled with ^{32}pCp using T4 RNA ligase. This viral RNA fragment is 386 nt in length, and contains sequence starting from R(+1) through the 18th codon of Gag. Thus, in addition to the 5′-UTR sequence, this RNA contains additional 54 nts of translated RNA, but for ease of reference, it will be referred to herein as the 5′-UTR RNA. 10 μl reaction mixtures containing 100 nM of ^{32}pCp-RNA substrate and varying amounts of indicated protein in binding buffer were incubated at room temperature for 1 h, and then dropped onto nitrocellulose membrane. The membranes were washed with binding buffer for three times, and then allowed to air dry. The signals were detected and quantitated using a PhosphorImager instrument.

2.13. Statistical analysis

Statistical analysis was performed by Student's *t* test. *P* value < 0.05 was considered significant and indicated with asterisks.

3. Results

3.1. The properties of mutant RHAs in RNA binding and unwinding

RHA contains two dsRBDs (dsRBD1 and dsRBD2) at the N-terminus (Fig. 1A). Each dsRBD contains two conserved lysine residues that have been found in dsRBD of other proteins (Fig. 1B) and homologs of RHA from other organisms (analyzed in Fig. 7). The conserved lysine residues of RHA are K54 and K55 in dsRBD1 and K235 and K236 in dsRBD2. While these lysine residues have been investigated using isolated dsRBDs [19,25,38], its activity in the context of enzymatically active full-length RHA is not known. Thus, we purified full-length mutant RHAs from mammalian cells, in which these conserved lysine residues were replaced by alanine in either dsRBD1, dsRBD2, or in both dsRBDs (Fig. 1A). In Fig. 1D, we show the electrophoretic analysis of the purified N-terminally His-tagged mutant RHA species. Purification of His-tagged wild-type RHA has been described [8]. We noticed two faint protein bands in Coomassie Brilliant Blue R250 staining analysis when protein loading was increased. We also found that these bands associate with Ni-NTA agarose rather than the purified proteins, thus they may represent the non-specific proteins that were co-purified by Ni-NTA agarose from 293E cell lysates. We measured the ability of mutant RHAs to bind and unwind synthetic duplex RNA. As shown in Fig. 2A, the short RNA strand in the duplex RNA is 3′-end labeled by [^{32}pCp]. Because the ability of RHA to recognize and bind substrate RNA is a prerequisite for the helicase activity of protein, we first determined the ability of mutant RHAs to bind to the duplex RNA by performing EMSA. As shown in Fig. 2B, both wild-type and mutant RHAs interact with the [^{32}pCp]-labeled RNA duplex, as indicated by the shift in probe mobility. The specificity of this interaction was evaluated by replacing the RHAs with GST, a non-RNA binding protein. The results show that both wild-type and mutant RHAs have the similar capability to bind duplex RNA *in vitro*.

We then determined the ability of mutant RHAs to unwind the radioactive duplex RNA in the presence of ATP, using EMSA to resolve duplex from single-stranded RNA (ssRNA). The [^{32}pCp]-labeled duplex RNA was incubated with indicated protein at 37 °C in the presence of 1 mM ATP. The unwinding reaction was stopped at the indicated time points by proteinase K digestion, and the reaction mixture was then separated in a native polyacrylamide gel. Unwinding activity will release the [^{32}pCp]-tagged short RNA strand from the duplex, producing a radioactive band of faster mobility in 1D PAGE. As shown in Fig. 2C, wild-type and mutant RHAs all have the ability, in the presence of ATP, to cause a decrease of duplex RNA accompanying an increase of ssRNA, indicating that each mutant RHA still possesses unwinding activity. We noted that RHA with mutations in both dsRBDs shows only a slightly slower rate of RNA unwinding (Fig. 2D). Reason for this phenomenon has yet to be investigated.

3.2. Ability of mutant RHAs to stimulate the accumulation of HIV-1 mRNAs

RHA has been reported to stimulate the accumulation of HIV-1 mRNA upon overexpression [5]. To elucidate the role of the conserved lysine residues in each dsRBDs in this viral process, 293T cells were cotransfected with SVC21.BH10 and plasmids coding for either wild-type or mutant RHAs. 24 h posttransfection, total cellular RNA was isolated and subjected to Northern blot analysis using [^{32}P]-labeled DNA probes that are complementary to the HIV-1 5′-UTR. The expression of exogenous wild-type or mutant RHAs was examined by Western blot analysis of cellular lysates using anti-RHA or anti-His (Fig. 3A). Fig. 3B shows that three different lengths of HIV-1 mRNA representing the multiply spliced ~1.8 kb (MS), singly spliced ~4.0 kb (SS), and unspliced ~9.2 kb (US) RNA species were detected by Northern blot analysis. Equivalent cellular RNA loading was confirmed by visualizing 18S and 28S ribosome RNAs after staining with ethidium bromide. The accumulation of all three classes of HIV-1 mRNAs was significantly increased by the coexpression of exogenous wild-type RHA, but much less so by the expression of mutant RHAs. Furthermore, semiquantitative RT-PCR analysis of total RNA using a specific primer set detected the comparable level of exogenous mRNAs encoding wild-type or mutant RHA that were produced from the cotransfected RHA constructs (Fig. 3C), suggesting the similar transfection efficiency. Thus, the

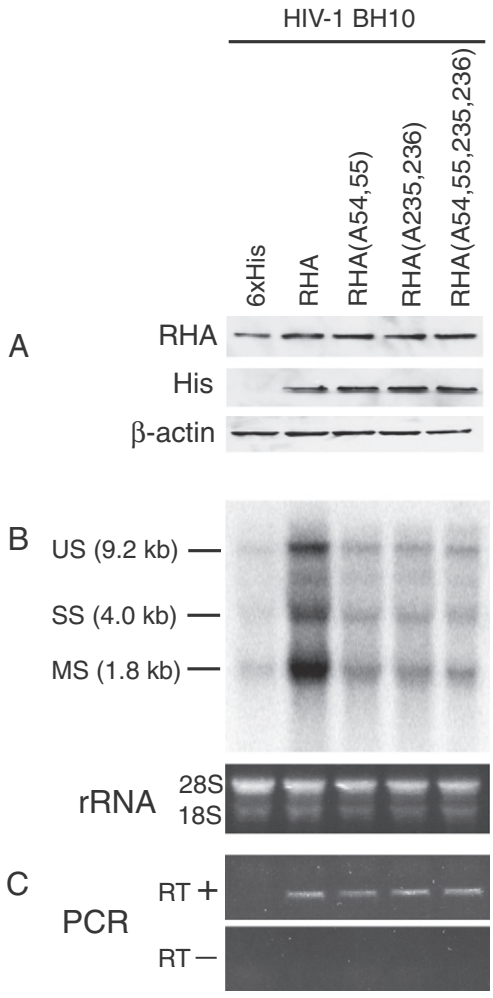

Fig. 3. Ability of mutant RHAs to stimulate the accumulation of HIV-1 mRNAs in the cell. 293T cells were cotransfected with SVC21.BH10 and a plasmid expressing either His-tagged wild-type or mutant RHA, or only the 6 × His tag. Western and Northern blots were analyzed at 24 h later. (A) Western blots of cell lysates probed with anti-RHA, anti-His, or anti-β-actin. (B) Northern blotting. The total cellular RNA was separated in a denaturing 1% agarose gel, blotted onto GeneScreen Plus membrane, and then probed with [^{32}P]-labeled DNA probes that are complementary to HIV-1 5′-UTR. Ethidium bromide-stained 18S and 28S rRNAs serve as RNA loading controls. Unspliced (US) ~9.2 kb, singly spliced (SS) ~4.0 kb, and multiply spliced (MS) ~1.8 kb RNA species are indicated. Shown is a representative of 3 independent experiments. (C) RT-PCR analysis of exogenous RHA-encoding mRNAs produced from cotransfected RHA constructs in the presence (+) or absence (−) of reverse transcriptase (RT).

difference in viral RNA accumulation was not a result from the varying transfection efficiency. Overall, the results indicate that the conserved lysine residues in dsRBD1 and dsRBD2 are all important for the stimulation of HIV-1 mRNA accumulation by RHA.

3.3. Ability of mutant RHAs to be incorporated into viral particles and to promote the annealing of tRNA^{Lys3} to viral RNA

RHA is packaged in HIV-1 particles [7,17]. Because dsRBDs have been shown to be necessary for the packaging of RHA into HIV-1 particles [16], we investigated whether the mutation of conserved lysine residues in dsRBDs can affect this process. First, siRNA$_{RHA}$ was used to knockdown the endogenous RHA in 293T cells. 16 h later cells were cotransfected with SVC21.BH10 and RHA constructs expressing either His-tagged wild-type or mutant RHAs. The siRNA$_{RHA}$ does not reduce the expression of exogenous RHAs as their mRNAs lack the siRNA$_{RHA}$ target sequence [8]. 48 h posttransfection, the extracellular viral particles were purified, and cellular and viral lysates were prepared. Western blots of cell lysates probed with anti-RHA verified that the siRNA$_{RHA}$ efficiently reduced the endogenous RHA in the cell, but did not affect the expression of exogenous wild-type or mutant RHAs, which were expressed at the comparable level in the presence of siRNA$_{RHA}$ (Fig. 4A). Western blots of viral lysates probed with anti-RHA or anti-His revealed that only wild-type exogenous RHA was readily detected in the virus particles (Fig. 4B). Thus, the

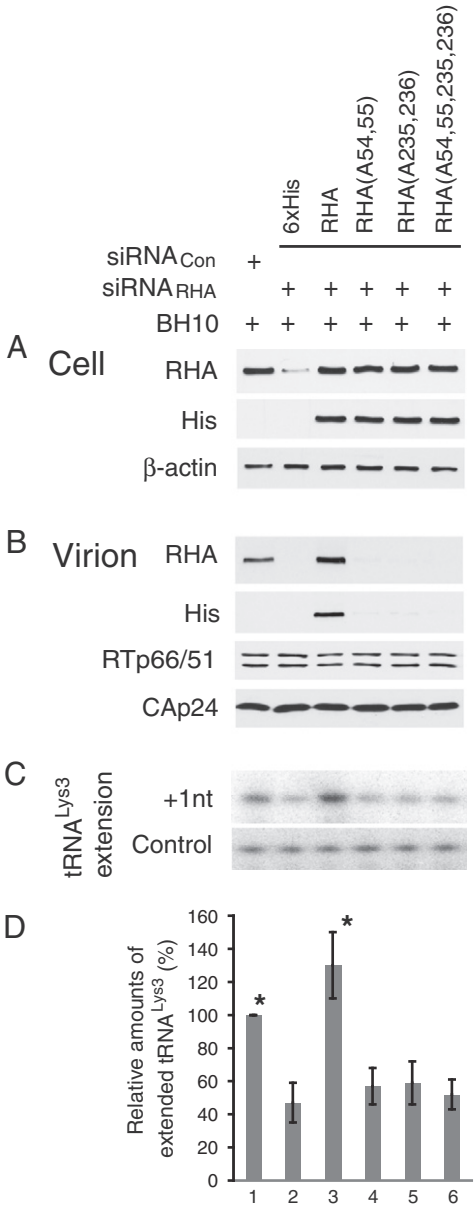

Fig. 4. Ability of mutant RHAs to be incorporated into viral particles and to promote the annealing of tRNA^{Lys3} to viral RNA. 293T cells were first treated with siRNA$_{Con}$ or siRNA$_{RHA}$, and 16 h later, were cotransfected with SVC21.BH10 and a plasmid expressing either 6 × His tag, or His-tagged wild-type or mutant RHA. 48 h later, extracellular viruses were purified. (A) Western blots of cell lysates probed with antibodies to RHA, His tag, or β-actin. (B) Western blots of viral lysates, containing equal amount of CAp24, probed with antibodies to RHA, His tag, CAp24, or RTp66/p51. (C) One nucleotide extension assay (+1 nt extension). Total viral RNA was isolated from purified HIV-1 particles, and tRNA^{Lys3} annealed to viral RNA was extended by 1 nt ([^{32}P]-dCTP), using HIV-1 reverse transcriptase. The extended tRNA^{Lys3} products were resolved by 1D PAGE, and detected using a PhosphorImager instrument. The control gel represents the +1 nt extension of a DNA primer annealed to viral RNA downstream of the tRNA^{Lys3} binding site, and is used to show that approximately equal amounts of viral RNA were used in each extension reaction. (D) The values of the +1 nt extended tRNA^{Lys3} products were quantitated using a PhosphorImager software, normalized to those values obtained with virions produced from siRNA$_{Con}$-treated cells (lane 1), and are presented graphically as percentage. Shown are the mean values ± SDs of 3 independent experiments. *, $P < 0.05$ compared with values obtained with virions produced from cells transfected with a plasmid expressing only His tag (lane 2).

mutation of the conserved lysine residues in either one or both of the dsRBDs significantly reduced the ability of RHA to be incorporated into virus particles.

The promotion of annealing of $tRNA^{Lys3}$ to viral RNA by RHA has been suggested to be associated with the remodeling of the secondary structure of HIV-1 5′-UTR [8]. The amount of $tRNA^{Lys3}$ annealed to viral RNA can be examined by a one nucleotide (nt) extension assay of the $tRNA^{Lys3}$ by reverse transcriptase [8]. In this assay, total viral RNA isolated from purified HIV-1 particles is deproteinized, and used as the source of primer $tRNA^{Lys3}$ annealed *in vivo* to viral genomic RNA. The incorporation of the first dNTP, [^{32}P]-dCTP, is detected by 1D PAGE. Using this assay, we previously reported that depletion of endogenous RHA by $siRNA_{RHA}$ reduced the annealing of $tRNA^{Lys3}$ to viral RNA, and that this defect in $tRNA^{Lys3}$ annealing can be rescued by the expression of exogenous RHA whose mRNA product lacks the $siRNA_{RHA}$ target sequences [8]. Since the mRNAs encoding the mutant RHAs in this report also lack $siRNA_{RHA}$ target sequence, the 1 nt extension assay was carried out to examine the ability of each mutant RHA to rescue reduced $tRNA^{Lys3}$ annealing by $siRNA_{RHA}$ (Fig. 4C, upper panel). Equal amounts of viral genomic RNA used in these reactions were first quantitated by dot blot hybridization, and further validated by a 1 nt extension of an annealed DNA primer complementary to viral RNA sequence downstream of the $tRNA^{Lys3}$ binding site (Fig. 4C, control panel). The 1D PAGE data shown in Fig. 4C were quantitated using a PhosphorImager software, Results are shown graphically in Fig. 4D. Normal annealing (lane 1) was reduced by the presence of $siRNA_{RHA}$ (lane 2), and rescued by exogenous wild-type RHA (lane 3), while much less rescue of annealing was obtained by the expression of the RHAs containing mutant dsRBDs (lanes 4–6). Thus, the results indicate that the conserved lysine residues in the dsRBDs are important for the promotion of $tRNA^{Lys3}$ annealing to viral RNA by RHA.

3.4. The binding of mutant RHAs to HIV-1 RNA in the cells

In order to clarify how the mutation of conserved lysine residues inhibited the RHA-stimulated processes during HIV-1 production, an RNA–protein coprecipitation assay was performed to assess the ability of mutant RHA to interact with HIV-1 RNA in the cells. 293T cells were cotransfected with SVC21.BH10 and plasmid constructs expressing His-tagged wild-type or mutant RHAs. Cotransfection with SVC21.BH10 and a plasmid expressing only the His tag served as a negative control. 24 h posttransfection, cells were formaldehyde cross-linked, lysed, and sonicated. Western blots of equal volumes of cell lysate probed with anti-His indicate comparable expression of wild-type and mutant RHAs (Fig. 5A). His-tagged wild-type and mutant RHAs were then precipitated from the cell lysates using Ni-NTA agarose. Western blots of column eluant probed with anti-RHA indicated roughly equal amounts of wild-type or mutant RHAs in the eluants (Fig. 5B). After deproteinization by TRIzol reagent, the total cellular RNA (as input before precipitation with Ni-NTA agarose) and RNA isolated from the precipitates were analyzed by RT-PCR with primer pair P1-F/R [16] that is specific for the 5′-UTR of HIV-1 RNA (Fig. 5C). Comparing with the corresponding input control, RT-PCR readily detected the HIV-1 transcripts containing sequence of 5′-UTR that were coprecipitated with wild-type RHA, but very little HIV-1 transcripts were detected in the mutant RHA precipitates. The results demonstrate that the mutation of the conserved lysine residues in either one or both of dsRBDs dramatically reduced the interaction of RHA with HIV-1 RNA during virus production.

3.5. In vitro binding of mutant RHAs to HIV-1 5′-UTR

The results obtained above show that mutant RHAs efficiently bind to short artificial RNA substrate *in vitro* (Fig. 2), but inefficiently bind to HIV-1 RNA in the cells (Fig. 5). Since the artificial duplex RNA used may lack the structural complexity that may be associated with more natural RNA substrates for RHA, we therefore investigated the activity

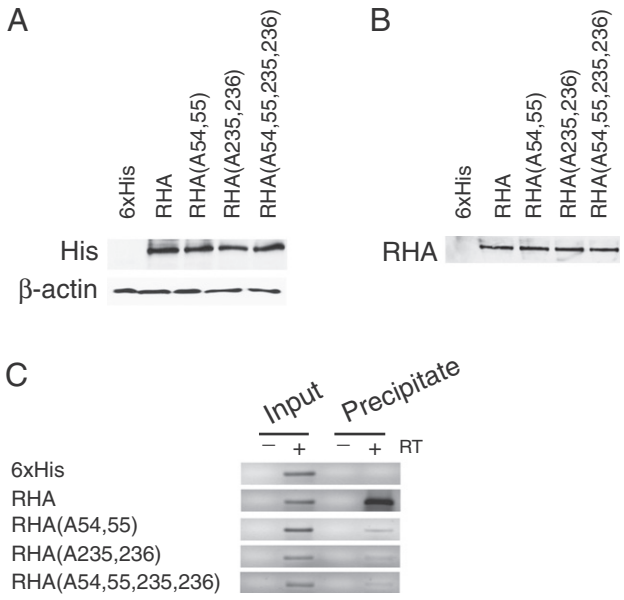

Fig. 5. Interaction of mutant RHAs with HIV-1 RNA in the cell. 293T cells were cotransfected with SVC21.BH10 and a plasmid expressing either His-tagged wild-type or mutant RHA, or only the 6 × His tag. 24 h later, cells were exposed to cross-linking, lysed, and sonicated. The wild-type or mutant RHAs in cell lysates were precipitated by Ni-NTA agarose. RNA was isolated from either cell lysates (input) or precipitates, and was analyzed by RT-PCR. (A) Western blots of cell lysates probed with anti-His detected expression of His-tagged proteins in the cells. The His-tag peptide alone was not detected in these Western blots. (B) Western blots of the precipitates obtained with Ni-NTA agarose, probed with anti-RHA. (C) Both input and coprecipitated RNAs were analyzed by RT-PCR, using primer pair P1-F/R specific to the HIV-1 5′-UTR. RT-PCR was performed in the presence (+) or absence (−) of reverse transcriptase (RT).

of these conserved lysine residues in the *in vitro* binding of RHA to a natural RHA substrate, the 5′-UTR of HIV-1 by performing RNA filter binding assay in which RNA bound to protein is retained on the filter. Binding of RHA to the 5′-UTR of HIV-1 genome has been shown to be associated with facilitating the transcription [5] and translation of viral mRNAs [7], and primer $tRNA^{Lys3}$ annealing [8]. This RNA contains multiple stem–loop structures including TAR-poly(A), PBS stem–loop, and leader regions of HIV-1 RNA [8,50]. GST does not bind to RNA, and was used as a negative control. As shown in Fig. 6, ^{32}pCp-tagged HIV-1 5′-UTR RNA was detected when either wild-type or mutant RHA was present, confirming the interaction of these proteins with the HIV-1 5′-UTR *in vitro*. Quantitative results in Fig. 6B show that none of the lysine mutations affected the ability of RHA to bind to this natural substrate RNA *in vitro*.

4. Discussion

In this report, we studied the activity of conserved lysine residues in dsRBDs of RHA in multiple steps of HIV-1 RNA metabolism and have shown that the substitution of the two conserved lysine residues in either dsRBD achieves similar results, *i.e.* significantly reduces the promotion by RHA of the accumulation of viral RNA (Fig. 3), the annealing of $tRNA^{Lys3}$ to viral RNA (Fig. 4C and D), and the incorporation of RHA into virion progeny (Fig. 4B). We also found that mutant RHAs containing these mutations are still capable to efficiently unwind dsRNA (Fig. 2). Thus, the inhibitory effects of mutation of the conserved lysine residues on tested HIV-1 processes would be mainly attributed to the dramatically reduced ability of RHA to interact with HIV-1 RNA in the cell (Fig. 5).

Biochemical and biophysical analyses of isolated dsRBDs identified amino acids including K54 and K55, and K235 and K236 that are critical to the binding of protein to RNA [19,25] as the mutation of those residues abolished the ability of isolated dsRBDs to bind RNAs containing

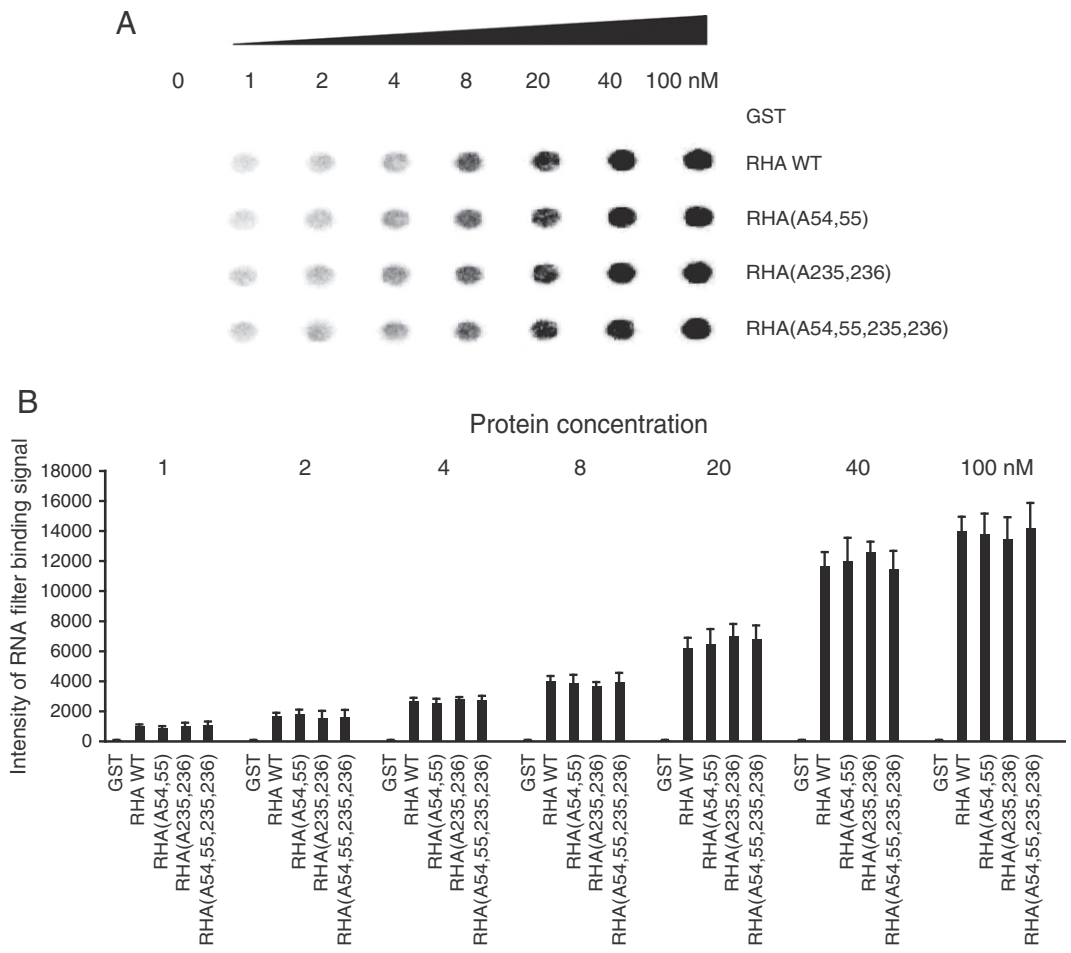

Fig. 6. *In vitro* binding of mutant RHAs to HIV-1 5′-UTR RNA. (A) RNA filter-binding assay was performed in triplicate to measure the binding of RHA to HIV-1 5′-UTR *in vitro*. The binding reaction contains 100 nM ^{32}pCp-labeled HIV-1 5′-UTR RNA and increasing amounts of purified proteins. GST was included as a non-RNA binding protein control. Reaction mixture was blotted onto nitrocellulose membrane followed by extensive washing. The radioactive signal was detected using a PhosphorImager instrument. (B) Quantitative results are shown as the mean values ± SD. Shown is a representative of 3 independent experiments.

double-stranded region [19,25,38]. By contrast, in the context of enzymatically active full-length RHA, we did not detect the effects of mutation of K54, K55, K235, and K236 in varying combinations on the binding affinity of protein for substrate RNA *in vitro* (Figs. 2 and 6). The discrepancy between this report and others possibly arises from the different sources of proteins analyzed, *i.e.* RHA of the full-length from mammalian cells used in this report *vs.* isolated dsRBDs from *E. coli* used elsewhere [19,25,38]. In addition to dsRBDs, other domains of RHA also have the ability to bind RNA, including the RGG domain in the C-terminus of RHA [23–25], OB-fold [26], and some motifs within the core helicase domain [22,51–53].

The observation that mutant full-length RHAs containing the substitution of the conserved lysine residues in dsRBDs have the similar capability as wild-type RHA to bind to HIV-1 RNA *in vitro* (Fig. 6) but show a dramatically reduced ability to interact with viral RNA in the cells (Fig. 5) may reflect the different RNA binding processes between *in vitro* and in the cell and suggest that cellular cofactors lacking in *in vitro* assay may modulate the binding of RHA to viral RNA in the cells. Since the dsRBDs have also been shown to play a role in the interaction between RHA and other proteins [54], we cannot eliminate the possibility that the effect of the lysine mutations on some functions of RHA may result from the disruption of such interactions. There are a number of examples of cofactors that can play a role in RHA function. For example, while a direct binding of RHA to a post-transcriptional control element (PCE) in the 5′-UTR of a set of RNAs has been proposed to be responsible for the RHA-stimulated translation, possibly due to a direct unwinding of the structurally complex 5′-UTR to allow more efficient ribosomal scanning [15], the work with other cellular mRNAs including those for type I collagen or those for Oct4, a human embryonic stem cell (hESC)-specific transcription factor responsible for maintaining stem cell pluripotency, suggests that the observed stimulation of translation of these mRNAs by RHA may involve RHA interacting directly with other mRNA binding proteins such as the collagen mRNA-binding protein, LARP6 [55], or the hESC-specific RNA binding proteins L1TD1 and Lin28, both of which can bind to Oct4 mRNA [55,56].

Using isolated dsRBDs of RHA, it was suggested that only dsRBD2 is involved in the *in vitro* binding of RHA to viral RNA, primarily with the TAR stem [5]. Our observation shows that both dsRBDs are required for the interaction between RHA and viral RNA in the cell [16]. Furthermore, as shown in Fig. 3, lysine substitution mutation in either dsRBD reduces RHA-stimulated accumulation of HIV-1 mRNA, implying a role for both dsRBDs in this process. The results of RHA are in contrast to a study of MLE (the RNA helicase maleless), an ortholog of RHA in *Drosophila melanogaster* (Fruit fly), reporting that the two dsRBDs in that protein (referred to as RB1 and RB2 respectively) are functionally distinct [57]. RB1 is critical for targeting MLE to the X chromosome *in vivo*, but has no ability to bind RNA, and its deletion has little effects on ATPase and helicase activities. RB2, however, is dominant for RNA binding, and is indispensable for ATPase and helicase activity. However, phylogenetic analysis using ClustalW2 [58] reveals that MLE is distantly related to human RHA and orthologs from other organisms (Fig. 7). Thus, the discrepancy between RHA and MLE may reflect their genetic distance.

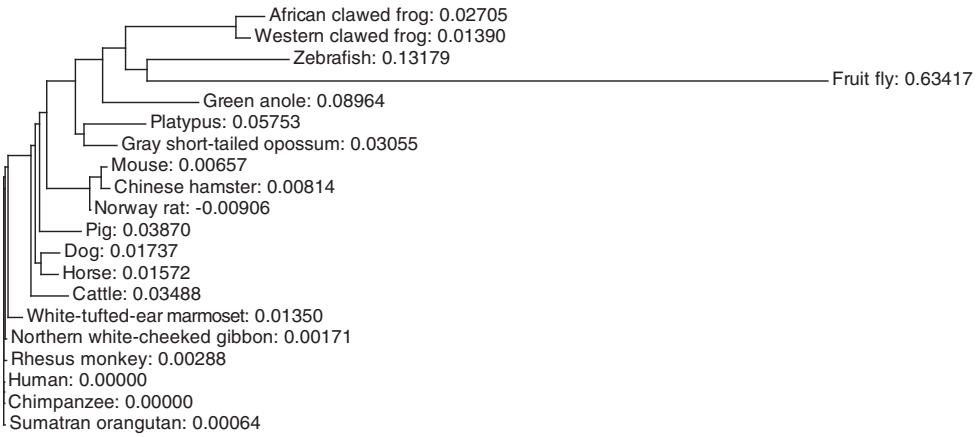

Fig. 7. Phylogeny of RHA from 20 different organisms was analyzed by ClustalW2 analysis. The numbers indicate the relative phylogenetic distance.

Acknowledgements

This work was supported by a grant from the Canadian Institutes of Health Research.

References

[1] Q.S. He, H. Tang, J. Zhang, K. Truong, F. Wong-Staal, D. Zhou, Comparisons of RNAi approaches for validation of human RNA helicase A as an essential factor in hepatitis C virus replication, J. Virol. Methods 154 (2008) 216–219.
[2] O. Isken, M. Baroth, C.W. Grassmann, S. Weinlich, D.H. Ostareck, A. Ostareck-Lederer, S.E. Behrens, Nuclear factors are involved in hepatitis C virus RNA replication, RNA 13 (2007) 1675–1692.
[3] P. Lawrence, E. Rieder, Identification of RNA helicase A as a new host factor in the replication cycle of foot-and-mouth disease virus, J. Virol. 83 (2009) 11356–11366.
[4] L. Lin, Y. Li, H.M. Pyo, X. Lu, S.N. Raman, Q. Liu, E.G. Brown, Y. Zhou, Identification of RNA helicase A as a cellular factor that interacts with influenza A virus NS1 protein and its role in the virus life cycle, J. Virol. 86 (2012) 1942–1954.
[5] R. Fujii, M. Okamoto, S. Aratani, T. Oishi, T. Ohshima, K. Taira, M. Baba, A. Fukamizu, T. Nakajima, A role of RNA helicase A in cis-acting transactivation response element-mediated transcriptional regulation of human immunodeficiency virus type 1, J. Biol. Chem. 276 (2001) 5445–5451.
[6] J. Li, H. Tang, T.M. Mullen, C. Westberg, T.R. Reddy, D.W. Rose, F. Wong-Staal, A role for RNA helicase A in post-transcriptional regulation of HIV type 1, Proc. Natl. Acad. Sci. U. S. A. 96 (1999) 709–714.
[7] C. Bolinger, A. Sharma, D. Singh, L. Yu, K. Boris-Lawrie, RNA helicase A modulates translation of HIV-1 and infectivity of progeny virions, Nucleic Acids Res. 38 (2010) 1686–1696.
[8] L. Xing, C. Liang, L. Kleiman, Coordinate roles of Gag and RNA helicase A in promoting the annealing of $tRNA^{Lys3}$ to HIV-1 RNA, J. Virol. 85 (2011) 1847–1860.
[9] S. Aratani, T. Oishi, H. Fujita, M. Nakazawa, R. Fujii, N. Imamoto, Y. Yoneda, A. Fukamizu, T. Nakajima, The nuclear import of RNA helicase A is mediated by importin-alpha3, Biochem. Biophys. Res. Commun. 340 (2006) 125–133.
[10] H. Fujita, T. Ohshima, T. Oishi, S. Aratani, R. Fujii, A. Fukamizu, T. Nakajima, Relevance of nuclear localization and functions of RNA helicase A, Int. J. Mol. Med. 15 (2005) 555–560.
[11] S.F. Anderson, B.P. Schlegel, T. Nakajima, E.S. Wolpin, J.D. Parvin, BRCA1 protein is linked to the RNA polymerase II holoenzyme complex via RNA helicase A, Nat. Genet. 19 (1998) 254–256.
[12] S. Aratani, R. Fujii, T. Oishi, H. Fujita, T. Amano, T. Ohshima, M. Hagiwara, A. Fukamizu, T. Nakajima, Dual roles of RNA helicase A in CREB-dependent transcription, Mol. Cell. Biol. 21 (2001) 4460–4469.
[13] T. Nakajima, C. Uchida, S.F. Anderson, C.G. Lee, J. Hurwitz, J.D. Parvin, M. Montminy, RNA helicase A mediates association of CBP with RNA polymerase II, Cell 90 (1997) 1107–1112.
[14] J.A. Toretsky, V. Erkizan, A. Levenson, O.D. Abaan, J.D. Parvin, T.P. Cripe, A.M. Rice, S.B. Lee, A. Uren, Oncoprotein EWS-FLI1 activity is enhanced by RNA helicase A, Cancer Res. 66 (2006) 5574–5581.
[15] T.R. Hartman, S. Qian, C. Bolinger, S. Fernandez, D.R. Schoenberg, K. Boris-Lawrie, RNA helicase A is necessary for translation of selected messenger RNAs, Nat. Struct. Mol. Biol. 13 (2006) 509–516.
[16] L. Xing, M. Niu, L. Kleiman, In vitro and in vivo analysis of the interaction between RNA helicase A and HIV-1 RNA, J. Virol. 86 (2012) 13272–13280.
[17] B.B. Roy, J. Hu, X. Guo, R.S. Russell, F. Guo, L. Kleiman, C. Liang, Association of RNA helicase A with human immunodeficiency virus type 1 particles, J. Biol. Chem. 281 (2006) 12625–12635.
[18] C.G. Lee, J. Hurwitz, A new RNA helicase isolated from HeLa cells that catalytically translocates in the 3′ to 5′ direction, J. Biol. Chem. 267 (1992) 4398–4407.
[19] S. Zhang, F. Grosse, Molecular characterization of nuclear DNA helicase II (RNA helicase A), Methods Mol. Biol. 587 (2010) 291–302.
[20] T.J. Gibson, J.D. Thompson, Detection of dsRNA-binding domains in RNA helicase A and *Drosophila* maleless: implications for monomeric RNA helicases, Nucleic Acids Res. 22 (1994) 2552–2556.
[21] A. Marchler-Bauer, S. Lu, J.B. Anderson, F. Chitsaz, M.K. Derbyshire, C. DeWeese-Scott, J.H. Fong, L.Y. Geer, R.C. Geer, N.R. Gonzales, M. Gwadz, D.I. Hurwitz, J.D. Jackson, Z. Ke, C.J. Lanczycki, F. Lu, G.H. Marchler, M. Mullokandov, M.V. Omelchenko, C.L. Robertson, J.S. Song, N. Thanki, R.A. Yamashita, D. Zhang, N. Zhang, C. Zheng, S.H. Bryant, CDD: a conserved domain database for the functional annotation of proteins, Nucleic Acids Res. 39 (2010) D225–D229.
[22] O. Cordin, J. Banroques, N.K. Tanner, P. Linder, The DEAD-box protein family of RNA helicases, Gene 367 (2006) 17–37.
[23] C.G. Burd, G. Dreyfuss, Conserved structures and diversity of functions of RNA-binding proteins, Science 265 (1994) 615–621.
[24] S. Zhang, F. Grosse, Domain structure of human nuclear DNA helicase II (RNA helicase A), J. Biol. Chem. 272 (1997) 11487–11494.
[25] A. Ranji, N. Shkriabai, M. Kvaratskhelia, K. Musier-Forsyth, K. Boris-Lawrie, Features of double-stranded RNA-binding domains of RNA helicase A are necessary for selective recognition and translation of complex mRNAs, J. Biol. Chem. 286 (2011) 5328–5337.
[26] H. Walbott, S. Mouffok, R. Capeyrou, S. Lebaron, O. Humbert, H. van Tilbeurgh, Y. Henry, N. Leulliot, Prp43p contains a processive helicase structural architecture with a specific regulatory domain, EMBO J. 29 (2010) 2194–2204.
[27] B. Tian, P.C. Bevilacqua, A. Diegelman-Parente, M.B. Mathews, The double-stranded-RNA-binding motif: interference and much more, Nat. Rev. Mol. Cell Biol. 5 (2004) 1013–1023.
[28] U. Kim, Y. Wang, T. Sanford, Y. Zeng, K. Nishikura, Molecular cloning of cDNA for double-stranded RNA adenosine deaminase, a candidate enzyme for nuclear RNA editing, Proc. Natl. Acad. Sci. U. S. A. 91 (1994) 11457–11461.
[29] P.E. March, J. Ahnn, M. Inouye, The DNA sequence of the gene (rnc) encoding ribonuclease III of *Escherichia coli*, Nucleic Acids Res. 13 (1985) 4677–4685.
[30] E. Meurs, K. Chong, J. Galabru, N.S. Thomas, I.M. Kerr, B.R. Williams, A.G. Hovanessian, Molecular cloning and characterization of the human double-stranded RNA-activated protein kinase induced by interferon, Cell 62 (1990) 379–390.
[31] A. Kharrat, M.J. Macias, T.J. Gibson, M. Nilges, A. Pastore, Structure of the dsRNA binding domain of *E. coli* RNase III, EMBO J. 14 (1995) 3572–3584.
[32] M. Bycroft, S. Grunert, A.G. Murzin, M. Proctor, D. St Johnston, NMR solution structure of a dsRNA binding domain from *Drosophila* staufen protein reveals homology to the N-terminal domain of ribosomal protein S5, EMBO J. 14 (1995) 3563–3571.
[33] A. Ramos, S. Grunert, J. Adams, D.R. Micklem, M.R. Proctor, S. Freund, M. Bycroft, D. St Johnston, G. Varani, RNA recognition by a Staufen double-stranded RNA-binding domain, EMBO J. 19 (2000) 997–1009.
[34] S. Nanduri, B.W. Carpick, Y. Yang, B.R. Williams, J. Qin, Structure of the double-stranded RNA-binding domain of the protein kinase PKR reveals the molecular basis of its dsRNA-mediated activation, EMBO J. 17 (1998) 5458–5465.
[35] H. Wu, A. Henras, G. Chanfreau, J. Feigon, Structural basis for recognition of the AGNN tetraloop RNA fold by the double-stranded RNA-binding domain of Rnt1p RNase III, Proc. Natl. Acad. Sci. U. S. A. 101 (2004) 8307–8312.
[36] Z. Wang, E. Hartman, K. Roy, G. Chanfreau, J. Feigon, Structure of a yeast RNase III dsRBD complex with a noncanonical RNA substrate provides new insights into binding specificity of dsRBDs, Structure 19 (2011) 999–1010.
[37] J.M. Ryter, S.C. Schultz, Molecular basis of double-stranded RNA–protein interactions: structure of a dsRNA-binding domain complexed with dsRNA, EMBO J. 17 (1998) 7505–7513.

[38] Q. Fu, Y.A. Yuan, Structural insights into RISC assembly facilitated by dsRNA-binding domains of human RNA helicase A (DHX9), Nucleic Acids Res. 41 (2013) 3457–3470.
[39] J. Blaszczyk, J. Gan, J.E. Tropea, D.L. Court, D.S. Waugh, X. Ji, Noncatalytic assembly of ribonuclease III with double-stranded RNA, Structure 12 (2004) 457–466.
[40] K.T. Jeang, V. Yedavalli, Role of RNA helicases in HIV-1 replication, Nucleic Acids Res. 34 (2006) 4198–4205.
[41] A. Ranji, K. Boris-Lawrie, RNA helicases: emerging roles in viral replication and the host innate response, RNA Biol. 7 (2010) 775–787.
[42] G. Cachianes, C. Ho, R.F. Weber, S.R. Williams, D.V. Goeddel, D.W. Leung, Epstein–Barr virus-derived vectors for transient and stable expression of recombinant proteins, Biotechniques 15 (1993) 255–259.
[43] E.F. Terwilliger, E.A. Cohen, Y.C. Lu, J.G. Sodroski, W.A. Haseltine, Functional role of human immunodeficiency virus type 1 vpu, Proc. Natl. Acad. Sci. U. S. A. 86 (1989) 5163–5167.
[44] P.L. Pham, A. Kamen, Y. Durocher, Large-scale transfection of mammalian cells for the fast production of recombinant protein, Mol. Biotechnol. 34 (2006) 225–237.
[45] M.K. Gorny, V. Gianakakos, S. Sharpe, S. Zolla-Pazner, Generation of human monoclonal antibodies to human immunodeficiency virus, Proc. Natl. Acad. Sci. U. S. A. 86 (1989) 1624–1628.
[46] F. Guo, J. Saadatmand, M. Niu, L. Kleiman, Roles of Gag and NCp7 in facilitating $tRNA^{Lys3}$ annealing to viral RNA in human immunodeficiency virus type 1, J. Virol. 83 (2009) 8099–8107.
[47] L. Xing, M. Niu, X. Zhao, L. Kleiman, Roles of the linker region of RNA helicase A in HIV-1 RNA metabolism, PLoS ONE 8 (2013) e78596.
[48] L. Xing, E. Kieff, Epstein–Barr virus BHRF1 micro- and stable RNAs during latency III and after induction of replication, J. Virol. 81 (2007) 9967–9975.
[49] I. Wong, T.M. Lohman, A double-filter method for nitrocellulose-filter binding: application to protein–nucleic acid interactions, Proc. Natl. Acad. Sci. U. S. A. 90 (1993) 5428–5432.
[50] R.S. Russell, C. Liang, M.A. Wainberg, Is HIV-1 RNA dimerization a prerequisite for packaging? Yes, no, probably? Retrovirology 1 (2004) 23.
[51] J.M. Caruthers, D.B. McKay, Helicase structure and mechanism, Curr. Opin. Struct. Biol. 12 (2002) 123–133.
[52] S. Granneman, C. Lin, E.A. Champion, M.R. Nandineni, C. Zorca, S.J. Baserga, The nucleolar protein Esf2 interacts directly with the DExD/H box RNA helicase, Dbp8, to stimulate ATP hydrolysis, Nucleic Acids Res. 34 (2006) 3189–3199.
[53] B. Schwer, T. Meszaros, RNA helicase dynamics in pre-mRNA splicing, EMBO J. 19 (2000) 6582–6591.
[54] A.J. Sadler, O. Latchoumanin, D. Hawkes, J. Mak, B.R. Williams, An antiviral response directed by PKR phosphorylation of the RNA helicase A, PLoS Pathog. 5 (2009) e1000311.
[55] Z. Manojlovic, B. Stefanovic, A novel role of RNA helicase A in regulation of translation of type I collagen mRNAs, RNA 18 (2012) 321–334.
[56] J. Jin, W. Jing, X.X. Lei, C. Feng, S. Peng, K. Boris-Lawrie, Y. Huang, Evidence that Lin28 stimulates translation by recruiting RNA helicase A to polysomes, Nucleic Acids Res. 39 (2011) 3724–3734.
[57] A. Izzo, C. Regnard, V. Morales, E. Kremmer, P.B. Becker, Structure–function analysis of the RNA helicase maleless, Nucleic Acids Res. 36 (2008) 950–962.
[58] R. Chenna, H. Sugawara, T. Koike, R. Lopez, T.J. Gibson, D.G. Higgins, J.D. Thompson, Multiple sequence alignment with the Clustal series of programs, Nucleic Acids Res. 31 (2003) 3497–3500.